ELSEVIER

Seminars in ULTRASOUND CT and MRI

PET and SPECT Imaging of Brain Tumors

Jessica Zhang, MD,* Katie Suzanne Traylor, DO,† and James M. Mountz, MD, PhD‡

Neuroimaging plays a vital role in the diagnosis and post-treatment assessment of brain tumors, aiding in treatment optimization, prognostication, and patient management. New clinical treatments have resulted in increased complexity of imaging interpretation, thus integrating complementary information from multiple imaging modalities (computed tomography, magnetic resonance imaging, and nuclear medicine) contributes to a thorough and more accurate evaluation. In review, we discuss current strategies of brain tumor imaging, specifically detailing the role of nuclear medicine single-photon emission computed tomography and positron emission tomography with utilization of both common and uncommon radiotracers in tumor grading, diagnosis, and treatment response.
Semin Ultrasound CT MRI 00:1-11

Introduction

The World Health Organization (WHO) classifies brain tumors as benign vs malignant, and then further subcategorizes malignant tumors into 4 grades based on histologic aggressiveness.[1] Both intra- and extra-axial masses are categorized based on cell origin, histology, immunophenotype, and molecular/cytogenetic profile.[2] The frequency of tumor subtypes is dependent on patient demographics. Gliomas account for 45% of all brain tumors and 90% of all primary brain malignancies with an incidence of 6-8 cases/100,000 people. Gliomas are the most common primary brain malignancy in patients over 20 years of age.[3,4] Overall, metastatic disease remains the most common adult brain tumor and is 10 times more common than primary malignancies.[4]

Accurate diagnosis is necessary for optimal treatment strategy,[5] and neuroimaging plays a vital role in diagnosis, prognostication, treatment planning, and management. Brain tumor evaluation begins with anatomic cross-sectional imaging utilizing computed tomography (CT) or magnetic resonance imaging (MRI).[6-8] The superior soft tissue contrast and multisequence capabilities of MRI, relative to CT, result in improved tissue characterization, localization, and assessment of extent.[6] This leads to an improved and tailored differential diagnosis, aiding in surgical and treatment planning.[1,7] Although MRI is the optimal imaging modality for tumor characterization, CT remains the initial imaging modality for new or progressive neurologic deficits due to widespread availability and rapid imaging acquisition capabilities. Additionally, CT is the preferred imaging modality for evaluating osseous structures[9] and when MRI is contraindicated (eg, pacemaker).[3,10]

Nuclear medicine (NM) modalities, namely single-photon emission computed tomography (SPECT) and positron emission tomography (PET), also have significant roles in neuroimaging of brain tumors. NM imaging is achieved by administration of a radiotracer that has a representative physiologic distribution throughout the body. Both SPECT and PET result in 3-dimensional imaging acquisitions. SPECT functions utilize photomultiplier tubes at multiple projections around the patient, recording gamma emissions from the biologically distributed radiotracer. PET imaging measures photon emissions from positron annihilation. PET detectors are individually composed of scintillator crystals and photomultiplier tubes and are arranged into detector rings.[11] SPECT's tomographic display of radiotracer distribution significantly improves the ability to localize abnormal uptake from normal physiologic uptake.[12] PET has similar capabilities with the added benefit of improved spatial resolution.[3]

Tc^{99m}-pertechnetate and $Gallium^{68}$-diethylenetriamine pentaacetic acid have excellent contrast resolution in the setting of blood-brain barrier (BBB) disruption; however, they are not commonly used due to lack of tracer distribution

*University of Pittsburgh Medical Center, Department of Radiology.
†University of Pittsburgh Medical Center, Department of Radiology, Neuroradiology Division, Pittsburgh, PA.
‡University of Pittsburgh Medical Center, Department of Radiology, Nuclear Medicine Division, Pittsburgh, PA.
Funding: The images in this manuscript were supported in part by the US National Institutes of Health research grant U01CA140230.
Address reprint requests to Katie Suzanne Traylor, DO, Neuroradiology Division, University of Pittsburgh Medical Center, 200 Lothrop Street, South Tower, 2nd Floor, Suite 200, Pittsburgh, PA 15213 E-mail: traylorks@upmc.edu

https://doi.org/10.1053/j.sult.2020.08.007
0887-2171/

specificity. Tracers with increased specificity due to uptake based on cellular or metabolic physiology, for example, Thallium^{201} and Fluoro^{18}-fluorodeoxyglucose (F^{18}-FDG), are now more commonly used.[13]

The main disadvantage of routine SPECT or PET is the lack of anatomic information, which is significantly alleviated with dual-modality hybrid systems: SPECT-CT, SPECT-MRI, PET-CT, and PET-MRI.[12,14] This improved anatomic detail aids biopsy precision and better delineates tumor margins vs adjacent edema, resulting in more accurate tumor volume and more refined treatment strategies.[3] PET and MRI can be integrated with a stereotactic neuro-navigational system for stereotactic biopsy, resulting in improved targeting and more accurate histologic diagnosis and radiotherapy planning.[7,15]

Diagnosis and Grading of Brain Tumors

In 2016, the WHO brain tumor classification system was updated, redefining, eliminating, and introducing various diagnoses. Advancements in molecular and genetic analysis have been incorporated into the 2016 update, supplementing tumor histology. Specifically, the gliomas category has been reorganized based on new understanding of genetic factors and neuroimaging advancements. For example, isocitrate dehydrogenase (IDH) defines adult infiltrating gliomas, which are subcategorized by the 1p/19q codeletion. In the absence of the IDH mutation, the diagnosis is IDH-wild type astrocytoma. In the presence of the IDH mutation, if the 1p/19q codeletion is present the diagnosis is oligodendroglioma and if it is absent the diagnosis is IDH-mutant astrocytoma. Accurately defining tumor genetics is critical, as the tumor genetics affect prognosis. For example, IDH-mutant gliomas, including WHO grade IV glioblastomas (GBM), have a better prognosis vs IDH-wild type gliomas.[16] Additionally, imaging biomarkers, such as necrosis and hypervascularity correlate with higher intra-axial tumor grade. For extra-axial brain tumors (eg, meningioma), contrast enhancement has not been shown to correlate well with tumor grade.[15] MR spectroscopy can detect oncometabolite 2-hydroxy-glutarate accumulation within tumor cells, which occurs in the presence of IDH mutations.[16]

SPECT and PET provide important information with regard to brain tumors, including metabolism, physiology, and functionality of the tumor, beyond the capabilities of anatomic imaging alone.[10] The variety of radiotracers utilized with SPECT and PET allows in vivo evaluation of metabolic and molecular processes, including glucose utilization, nucleoside and amino acid transporter expression, and both protein and DNA synthesis.[8] Moreover, SPECT and PET can play a critical role in differentiating tumor from potential non-neoplastic mimics. A classic diagnostic imaging conundrum is the diagnosis of central nervous system (CNS) lymphoma vs toxoplasmosis. Both CNS pathologies have similar diagnostic imaging characteristics, often presenting as multiple ring-enhancing lesions in immunocompromised patients, making definitive diagnosis challenging. Utilization of F^{18}-FDG PET and Thallium^{201} SPECT leads to a definitive diagnosis, mandatory for patient treatment.[15]

In tumor evaluation, the ideal radiotracer has a high affinity for the tumor and low affinity for normal brain parenchyma.[3] Advances in NM imaging have resulted in increasing capabilities for specific molecular targets.[12,17]

SPECT

Radiotracers utilized for SPECT brain imaging include Thallium^{201}, Technetium(Tc)^{99m}-sestamibi (MIBI), Tc^{99m} ethyl-cysteinate dimer, Tc^{99m}-tetrofosmin, Iodine^{123}-alpha-methyl-tyrosine, and Indium^{111}-pentetreotide.[3] Thallium^{201} is a potassium analog actively transported into viable cells via a sodium potassium adenosine triphosphate cell membrane pump. This pump requires cell viability in order to accumulate radiotracer. Thallium^{201} uptake is independent of the BBB and based solely on rate of cell growth, and as a result is relatively specific for brain tumors.[3] A retrospective study of 90 patients found that Thallium^{201}-SPECT has a sensitivity of 71.7% and a specificity of 80.9% for supratentorial brain tumors.[18] Thallium^{201} accumulates in brain malignancies without significant uptake in normal brain parenchyma, as tumor growth rates are significantly higher resulting in excellent tumor-to-background contrast[3] (Figs. 1 and 2). The Thallium-threshold-index can be determined from early and delayed imaging. Non-neoplastic processes (eg, toxoplasmosis) demonstrate early uptake and washout due to lack of a cellular component.[3,19] In patients with primary or metastatic brain tumors, this index can help distinguish low- vs high-grade neoplasms.[3] A study of 34 patients with GBM and low-grade astrocytoma found low-grade malignancies to have a tumor-to-normal tissue ratio of below 1.5 while GBMs had a ratio of 2.5 or higher.[20]

Tc^{99m}MIBI is a synthetic lipophilic cation complex utilizing active diffusion to cross the BBB and concentrate in the mitochondria. MIBI uptake reflects perfusion and cellular activity and does not accumulate in nonviable cells.[2] Additionally, there is negligible MIBI uptake in the normal brain with only minimal uptake corresponding to the parotid

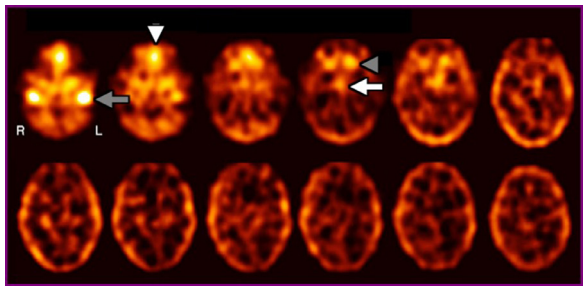

Figure 1 Thallium^{201} distribution in normal brain. Axial SPECT images show distribution of Thallium^{201} in normal brain. Note uptake in the parotid glands (gray arrow), ethmoid sinuses (white arrowhead), lacrimal gland (gray arrowhead), and the pituitary gland (white arrow).

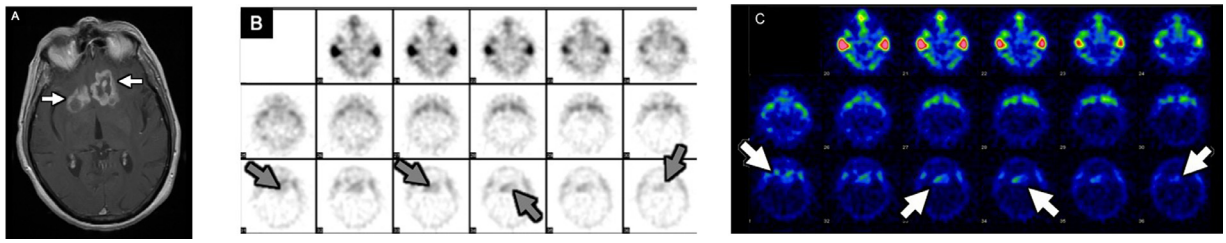

Figure 2 CNS lymphoma on Thallium^{201} SPECT. Axial postcontrast T1-weighted MRI (A) demonstrates irregular ring enhancing lesions in the bilateral inferior frontal lobes (white arrows). Sequential axial Thallium^{201} SPECT images (B – grayscale, C – color scale) show focal increased thallium uptake in these regions (gray and white arrows), consistent with lymphoma.

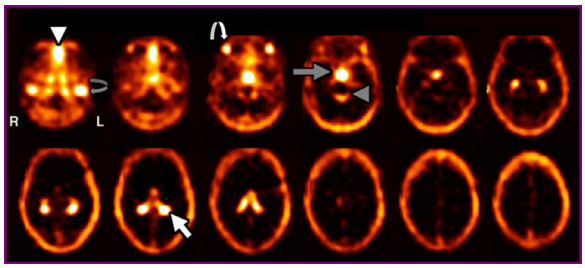

Figure 3 MIBI distribution in normal brain. Axial SPECT images showing the distribution of Tc^{99m} MIBI in normal brain. Note uptake in the parotid glands (curved gray arrow), ethmoid sinus (white arrowhead), lacrimal gland (curved white arrow), basal cistern cerebrospinal fluid (gray arrowhead), pituitary gland (gray arrow), and choroid plexus (white arrows).

glands, ethmoid sinus mucosa, lacrimal glands, cerebrospinal fluid, pituitary gland, and choroid plexus (Fig. 3). In determining viable tumor vs radiation necrosis (RN) following treatment, studies found accuracies of 95% for low-grade-treated gliomas and 87% for high-grade-treated gliomas on MIBI-SPECT.[3]

Both Tc^{99m}MIBI and Thallium^{201} have high tumor-to-background ratios; however, MIBI has a higher signal-to-noise ratio with improved edge definition. Like F^{18}-FDG and Thallium^{201}, MIBI can differentiate lymphoma from toxoplasmosis in immunocompromised patients.[2] In the evaluation of primary gliomas, MIBI uptake tends to correlate with tumor grade, although this correlation is more challenging with GBM due to tumor/necrosis heterogeneity (Fig. 4). Small paraventricular masses are difficult to detect using Tc^{99m} MIBI given the normal physiologic uptake/secretion by the choroid plexus[2] (Fig. 3).

Another synthetic lipophilic cation complex is Tc^{99m}-tetrofosmin, which like MIBI utilizes active diffusion; however, uptake is also dependent on membrane potentials. Uptake is proportional to regional blood flow, and radiotracer only localizes in viable tumor cells. Normal physiologic uptake of Tc^{99m}-tetrofosmin (choroid plexus, temporalis muscles, extraocular muscles, and dural venous sinuses) can obscure regional tumor evaluation, especially in the posterior fossa.[3] The use of hybrid SPECT-CT helps overcome this potential pitfall.[2]

Iodine^{123}-alpha-methyl tyrosine (IMT) is an amino acid labeled radiotracer that crosses the BBB via an amino acid transport carrier system. IMT has significant uptake in gliomas with little or no uptake in the normal brain parenchyma; thus, it helps distinguish viable tumor from RN. Although IMT-SPECT can be used as an alternative to FDG-PET, the significantly lower spatial resolution of SPECT vs PET hinders widespread utilization.[15-17,21,22] IMT-SPECT can also help define brain tumor volume and delineate accurate target volumes for radiation planning.[15]

Indium^{111}-pentetreotide binds to somatostatin receptors (SSRs), which are abundant in the basal ganglia, limbic system, and cortex. However, this tracer cannot cross the BBB, limiting usefulness for intra-axial tumors unless the BBB is disrupted. Intracranial tumors expressing SSRs include pituitary adenomas, meningiomas, oligodendrogliomas, and

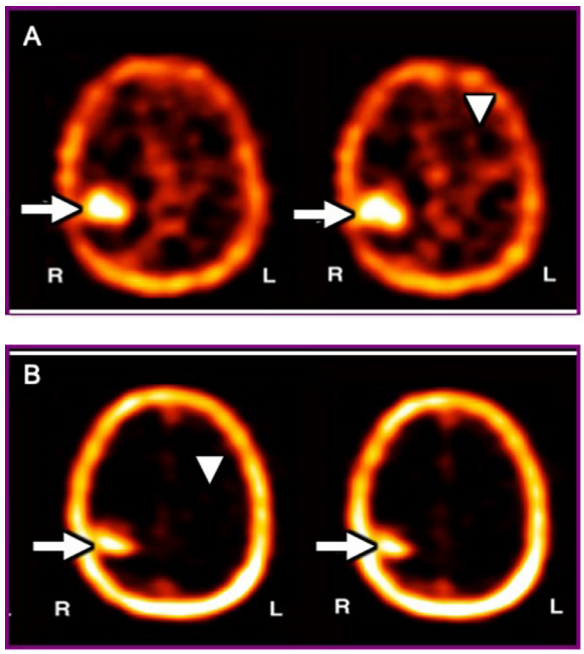

Figure 4 High-grade CNS tumor on Thallium^{201} and MIBI SPECT. Axial Thallium^{201} (A) and Tc^{99m} MIBI (B) SPECT images show elevated uptake correlating to the known high-grade right parietal CNS tumor (white arrows). Note that the low brain background uptake (white arrowheads) allows for a greater degree of distinction compared to what might be seen on F^{18}-FDG PET.

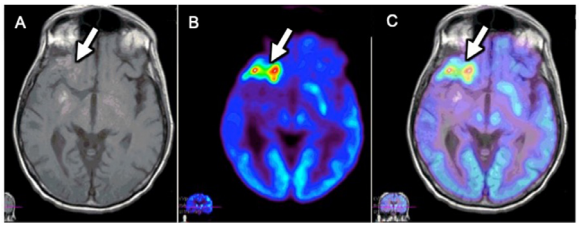

Figure 5 High-grade CNS tumor on FDG-PET and MRI. Axial FLAIR MRI (A), F^{18}-FDG PET (B), and fused F^{18}-FDG PET-MRI (C) images show corresponding patchy signal abnormality (white arrow) and intense FDG uptake greater than normal gray matter in the right frontotemporal region (white arrow), indicating high-grade tumor.

medulloblastomas.[23] Since pituitary adenomas and meningiomas are extra-axial, these lesions display elevated uptake.[3] Indium^{111}-pentetreotide can differentiate meningiomas from schwannomas and optic nerve sheath meningiomas from granulation tissue, as schwannomas and granulation tissue do not exhibit uptake.[3,12] Non-CNS tumors expressing SSRs include neuroendocrine tumors, carcinoids, paragangliomas, medullary thyroid carcinomas, pheochromocytomas, and small-cell lung cancers. Intracranial metastases from any of these SSR-expressing tumors can also show elevated uptake.[3]

PET

Aerobic glucose metabolism is the brain's primary energy source. F^{18}-FDG, the most utilized PET radiotracer, is actively transported across the BBB and accumulates in regions of increased aerobic glucose metabolism.[4,6] The intracellular concentration of FDG is proportional to glucose metabolism, and increased accumulation corresponds to high cellular metabolism.[4] The normally high metabolic activity of the brain results in high uptake in normal brain parenchyma, therefore low tumor-to-brain contrast. Another potential pitfall is the nonspecific nature of FDG uptake such that inflammatory/infectious processes also show elevated uptake.[22] Finally, high-grade tumors may have internal necrosis leading to decreased FDG uptake[6] (Fig. 5). Studies have shown that more delayed scanning results in increased FDG retention by tumor, thus higher tumor-to-background contrast.[10]

In addition to necrosis, both peritumor-associated cerebral diaschisis and tumoral edema can manifest decreased FDG uptake. Cerebral and crossed cerebellar diaschisis can be identified on PET or SPECT[6] (Fig. 6). Hypermetabolic tumors associated with diaschisis have lower median survival rate (7 months) vs those without diaschisis (33 months).[15]

PET radiolabeled amino acids utilize facilitated transport and accumulate proportionally to cellular proliferation.[4] Tumors cause transporter upregulation, increased metabolic enzyme activity, and increased demand, leading to increased radiotracer accrual proportional to protein synthesis and nutrient demand.[6] This accumulation correlates to tumor grade and treatment response.[15] PET radiolabeled amino acids, including Carbon^{11}-methionine (C^{11}-MET), F^{18}-fluoro-ethyl-tyrosine (F^{18}-FET), and L-3,4-dihyodroxy-6-[F^{18}] phenylalanine (F^{18}-DOPA), cross the BBB via transporters.[8,15] Although it is the most commonly studied radiolabeled amino acid, C^{11}-MET has limited clinical usage due to its 20-minute half-life and dependence on an on-site cyclotron. F^{18}, with its longer 110-minute half-life, is more commercially available.

The labeled amino acids F^{18}-DOPA and F^{18}-FET, as well as the labeled thymidine nucleoside analog F^{18}-flurothymidine (F^{18}-FLT), have similar functionality, higher tumor detection, and excellent tumor-to-brain contrast[6,22] (Fig. 7). F^{18}-FET uptake correlates to prognosis and is used for kinetic analysis of tumor proliferation in high-grade gliomas; pitfalls can arise where nonmalignant etiologies have uptake due to BBB disruption.[6,19] Amino acid and nucleoside-labeled radiotracers correlate to tumor angiogenesis and can show disproportionate amounts of uptake compared to the degree of tumoral enhancement on MRI or CT.[6] Their specific advantage over F^{18}-FDG is the low background uptake, increasing conspicuity of even low-grade tumors.[6] Studies have shown improved patient survival when resection is based on C^{11}-MET PET tumoral uptake vs only the

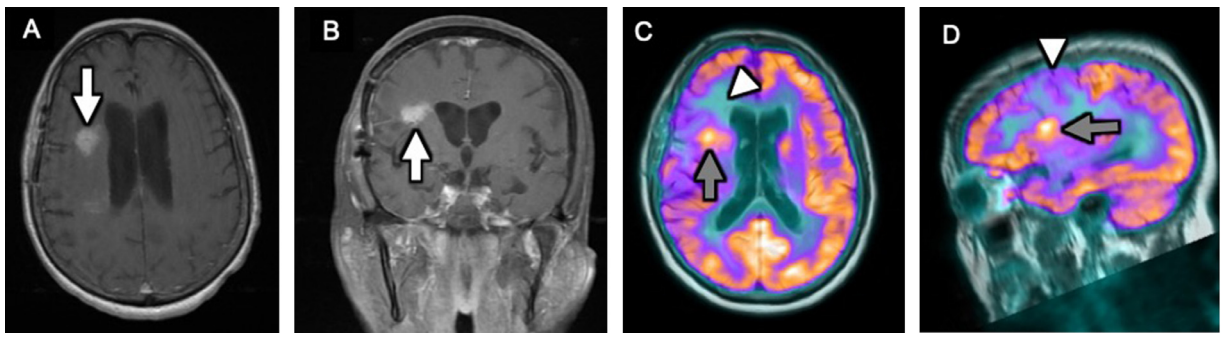

Figure 6 Diaschisis associated with biopsied glioma on FDG-PET and MRI. Axial (A) and coronal (B) postcontrast T1-weighted MR images demonstrate postprocedural changes and enhancement of the right frontal corona radiata (white arrow) in a patient with MGMT promoter methylated IDH wild type glioma. Axial (C) and sagittal (D) fused F^{18}-FDG PET-MRI show focal increased F^{18}-FDG uptake in the right frontal corona radiata (gray arrow), consistent with viable high-grade tumor. Surrounding area of decreased radiotracer uptake (white arrowheads) correspond to vasogenic edema and diaschisis.

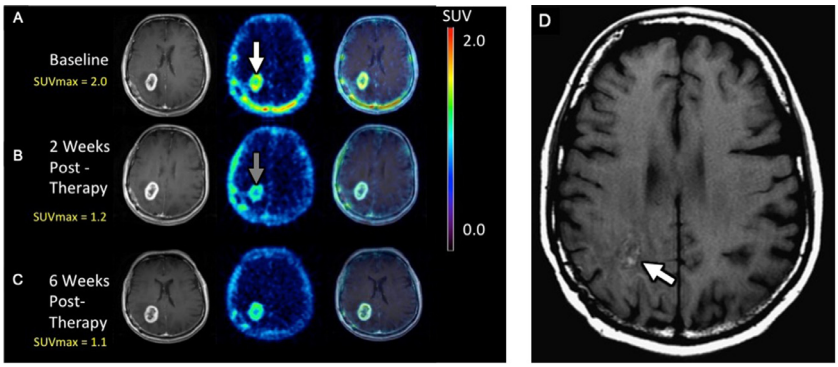

Figure 7 Tumor response on FLT-PET. Patient with GBM treated with 6 weeks of temozolomide and radiation treatment. Postcontrast axial MRI, F^{18}-FLT-PET, and fused PET-MRI exams pretreatment (A), at 2 weeks of therapy (B), and at 6 weeks of therapy (C). At baseline, the tumor showed elevated F^{18}-FLT uptake (white arrow). At the 2-week early response assessment time, MRI showed no substantial change; however, the F^{18}-FLT uptake was markedly reduced (gray arrow). At 6 weeks of therapy, sustained reduction of FLT uptake suggests the reduced uptake at 2 weeks accurately predicted a long-term good response. Note MRI is essentially unchanged from baseline at both the 2-week and 6-week follow-up timepoints. Axial postcontrast T1-weighted MRI at 4 months (D) shows significantly decreased enhancement (white arrow), confirming good response.[37] Images adapted with permission from "Assessment of early therapy response with 18F-FLT PET in glioblastoma multiforme," by Oborski, MJ et al, *Clin Nucl Med*, 39(10):e431-432.

enhancing component on anatomic imaging.[15] Although after gross total tumor resection F^{18}-FDG PET may be negative, uptake may be elevated on C^{11}MET PET, signifying the presence of residual tumor.[24]

F^{18}-fluoromisonidazole (FMISO) is a marker of hypoxia, which is a promoter of tumor angiogenesis.[6,15] FMISO is independent of the BBB and rapidly equilibrates within tissues irrespective of perfusion, becoming entrapped in viable cells located in a highly hypoxic environment.[6] Tumor hypoxia is due to the high proliferation rate and imbalanced blood supply of high-grade tumors such as GBM.[15] Therefore, FMISO can differentiate high- and low-grade gliomas, with improved characterization vs FDG.[10] Hypoxia is known to be radiation resistant, thus FMISO potentially can significantly impact treatment decisions.[1]

Lastly, routine $Gallium^{68}$-labeled somatostatin analog PET tracers include DOTA-TATE, DOTA-TOC, and DOTA-NOC. These are commonly used in the setting of metastatic well-differentiated neuroendocrine tumors of gastroenteric origin (eg, pancreas or small bowel).[25] DOTA-PET targets the SSR subtype-2, with similar biodistribution to its SPECT radiotracer counterparts, but with improved lesion-to-background contrast due to higher detected photon counts. DOTA-PET is helpful in both treatment planning and radiotherapy in nonsurgical patients with SSR-expressing brain tumors, such as meningiomas[6,15,25] (Fig. 8).

Treatment Response and Post-Treatment Imaging of Brain Tumors

Surgery remains the standard of care for brain tumors, and patient treatments are based on tumor histology and feasibility/safety of resection.[25-27] Different radiation treatments, such as stereotactic radiosurgery or whole-brain radiation, are selected depending on tumor type and multiplicity.[4] Additional therapies are often utilized, including steroids, intravenous chemotherapies, and intrathecal chemotherapy agents.[26] New chemotherapy and immunotherapy agents are continuously being developed, which may have drug-specific implications on the tumor and the imaging findings in the post-treatment setting.[27]

Neuroimaging is the primary tool in the evaluation of treatment efficacy and tumor response.[5] With the increasing number of treatments available, imaging interpretation has become increasingly challenging. Knowledge of tumor pathology, molecular phenotype, and treatment history are essential for interpretation, as the imaging appearance can reflect residual tumor, recurrence, or post-treatment effects.[10] Neuroimaging is ideally completed 24 hours post-resection to better assess residual tumor vs postsurgical granulation tissue.[7] After completion of radiotherapy, postradiation changes can lead to heterogeneous imaging appearances based on treatment timeframe—acute (days to weeks), early-delayed (weeks to months), or late-delayed (months to years), with RN known to occur after 6 months.[27]

Acute to early-delayed radiation changes result in BBB and vascular permeability alterations causing various enhancement patterns which differ from pretreatment imaging.[27] Post-treatment enhancement is challenging to discern from tumor on conventional anatomic imaging alone.[3] Postradiation edema and T2-signal abnormalities are often indistinguishable from tumoral edema and nonenhancing tumor on MRI.[26,27] Radiation also results in white matter and deep cortical signal abnormalities, related directly to radiation dose.[27] White matter is particularly susceptible to chemotherapy and can manifest as symmetric confluent T2-signal abnormality.[26,27] Given the imaging overlap, the presence of residual

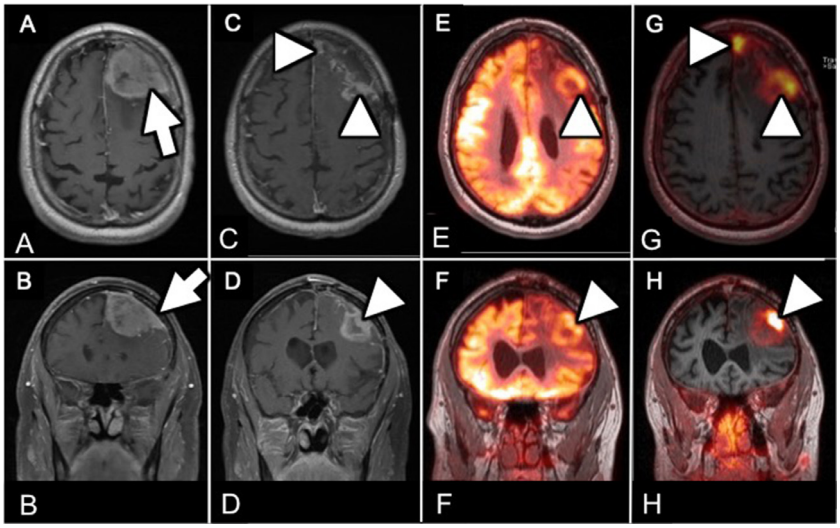

Figure 8 Recurrent anaplastic meningioma on FDG and Gallium^{68}-DOTA-TATE-PET. Axial (A) and coronal (B) postcontrast T1-weighted MRI shows a large enhancing left frontal WHO grade 3 anaplastic meningioma (white arrows). After stereotactic radiosurgery, axial (C) and coronal (D) postcontrast T1-weighted MR images show persistent enhancement in the treatment bed (white arrowheads). There is corresponding focal increased uptake (white arrowheads) on fused axial (E) and coronal (F) F^{18}-FDG PET-MRI, indicating viable high-grade tumor. Subsequently performed axial (G) and coronal (H) fused-Gallium^{68} DOTA-TATE PET-MR images show intense uptake (white arrowheads) in the left frontal region, corresponding to the previously documented regions of elevated FDG uptake and MRI enhancement. This indicates SSRs within the residual anaplastic meningioma, therefore potential benefit in SSR radionuclide therapies.

or recurrent tumor with superimposed treatment changes leads to interpretation challenges.[28] Moreover, postradiation changes in the brain are not limited to primary brain tumors, but can also occur following treatment of extracranial and extra-axial tumors, such as nasopharyngeal carcinomas and meningiomas.[29]

"Pseudoprogression" and "pseudoresponse" are potential postradiation imaging appearances that lead to diagnostic challenges. "Pseudoprogression" occurs during the first 6 months after therapy, typically within 3 months, and most commonly transpires in tumors with 6-O-Methylguanine-DNA Methyltransferase (MGMT) promoter methylation. Imaging resembles tumor progression with increased size, edema, and enhancement; however, these findings are related to tumor treatment response and correspond to improved prognosis and survival.[1,10,26,30] "Pseudoresponse" appears as significantly decreased tumoral enhancement post-treatment and is most commonly seen with antiangiogenic drugs such as bevacizumab, an anti-VEGF antibody medication.[5,26] These medications inhibit angiogenesis and decrease BBB permeability resulting in decreased mass effect and symptomatology; however, prognosis remains unchanged.[30]

MRI assessment of CNS tumor response was historically based on the 1990 Macdonald criteria, utilizing 2-dimensional measurements of enhancing tumor and neurologic status. However, there were many limitations such as no clear definition of progression, pseudoprogression, or pseudoresponse, and no consideration for nontumoral enhancement. The Response Assessment in Neuro-Oncology (RANO) multidisciplinary international working group was created to address these pitfalls and to standardize the criteria for treatment response. RANO also uses 2-dimensional tumor measurements but includes definitions of progression for trial enrollment and measurable disease. RANO addresses pseudoprogression by excluding recurrent disease occurring within the first 12-weeks of radiation, unless there is definitive recurrence outside the radiation field or histologic confirmation. Pseudoresponse is addressed by requiring confirmatory imaging in patients having received antiangiogenic medications no earlier than 4 weeks after finding a partial or complete response. There are also recommendations for equivocal post-treatment imaging appearances; however, issues persist with differentiation of nonenhancing tumor, postradiation changes, and ischemic injury. RANO attempts to account for nonenhancing tumor growth in its definition of tumor progression, but no objective criterion is provided.[31]

Despite advanced MRI sequences, such as MR perfusion and spectroscopy, PET and SPECT have complementary roles in providing physiologic information and can help differentiate RN from tumor.[15] Hybrid imaging of CT or MRI with PET or SPECT allows a better differentiation of post-treatment changes vs residual/recurrent tumor (Fig. 9). Methods include fusion of PET or SPECT images with postoperative MRI or stereotactic CT images, which identify sites of residual/recurrent tumor[26] (Figs. 10 and 11).

SPECT

SPECT is a relatively low-cost imaging modality, is widely available,[32] and is complementary to CT and MRI in the

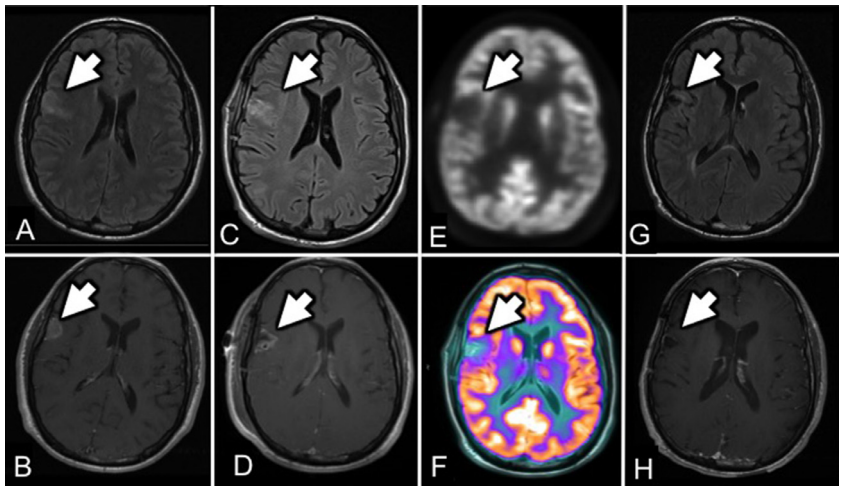

Figure 9 Postoperative changes with subsequent resolution on PET-MRI. Pretreatment MRI (A and B) in a patient with multifocal high-grade glioma shows multifocal cortical areas of mass like signal abnormality on axial FLAIR (A, white arrow) with associated enhancement on postcontrast T1-weighted imaging (B, white arrow). Postoperative MR images (C and D) demonstrate persistent FLAIR hyperintensity (C, white arrow) in the surgical bed with associated peripheral enhancement (D, white arrow). Axial PET (E) shows absent F^{18}-FDG uptake (white arrow) and fused axial PET-MRI (F) is helpful in localizing the absent F^{18}-FDG uptake to the region of previously seen signal abnormality (white arrow), which suggests post-treatment changes rather than recurrent or residual viable tumor. One-year postsurgery (G and H), the resection cavity exhibits decreased extent of FLAIR signal hyperintensity (G, white arrow) and contrast enhancement (H, white arrow).

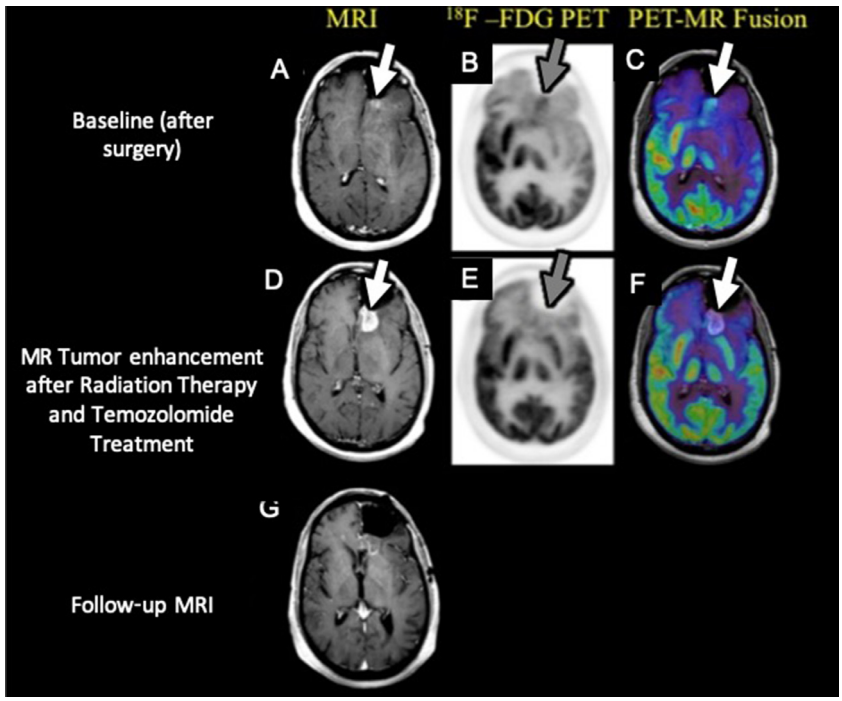

Figure 10 Pseudoprogression on FDG-PET. Patient with history of GBM. Initial postresection axial postcontrast T1-weighted MRI (A) shows mildly enhancing residual tumor (white arrow). Axial F^{18}-FDG PET (B) shows mildly elevated FDG uptake (gray arrow), which localizes to the area of enhancement on axial fused PET-MRI (C, white arrow). Following 10 weeks of therapy with temozolomide plus radiation therapy, follow-up MRI (D) shows increased enhancement (white arrow) suspicious for progression. As there was clinical improvement in symptoms, FDG-PET was performed. Axial attenuation correction F^{18}-FDG PET (E) shows no FDG uptake (gray arrow) and fused PET-MRI better localizes the hypometabolic focus to the area of increased enhancement (white arrow). Physiologic activity of F^{18}-FDG PET indicated that the MRI findings were related to pseudoprogression, thus additional therapy was withheld. Follow-up MRI at 4 months (G) and at 1 year (not shown) are negative, supporting the early diagnosis of pseudoprogression.[38] Images adapted with permission from "Distinguishing pseudoprogression from progression in high-grade gliomas: a brief review of current clinical practice and demonstration of the potential value of 18F-FDG PET" by Oborski, MJ et al, 2013, *Clin Nucl Med*, 38(5):381-384.

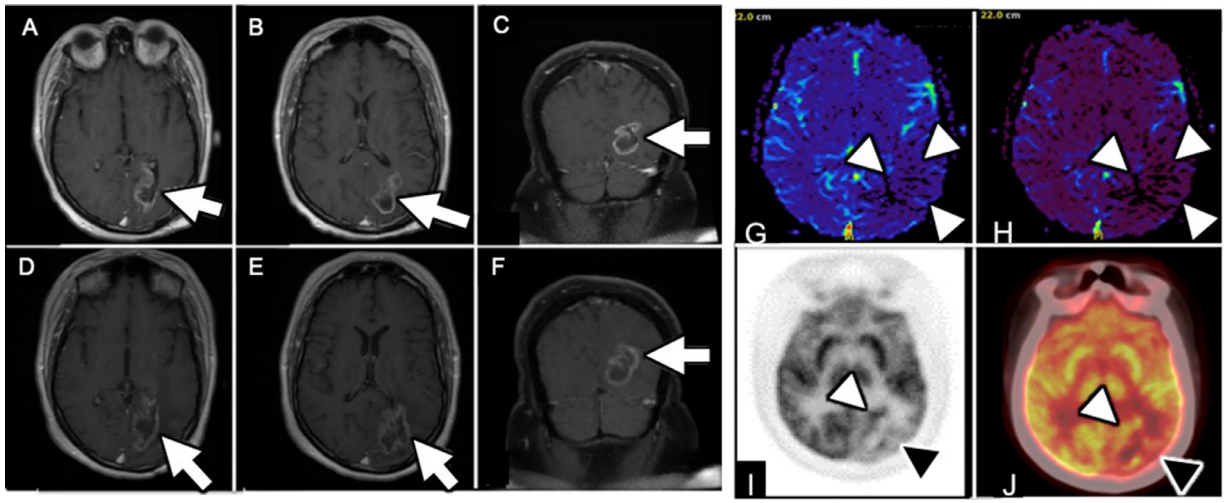

Figure 11 Recurrent GBM on PET-CT. Following gross resection of left occipital lobe IDH-wild type MGMT promoter methylated GBM in a patient on involved field radiation and concurrent temozolomide, baseline axial (A and B) and coronal (C) postcontrast T1-weighted MR images show significant enhancement (white arrows) within the resection cavity and left lateral ventricle subependymal region. MRI performed 9 months later (D, E, and F) shows increased extent of enhancement (white arrows), however without increased cerebral blood flow (G, white arrowheads) or cerebral blood volume (H, white arrowheads) on the corresponding the dynamic susceptibility enhanced MR perfusion images, favoring radiation injury. Due to clinical concern, F^{18}-FDG PET-CT was performed with axial attenuation corrected PET image (I) and PET-CT fused image (J) showing multiple areas of focal increased FDG uptake (white arrowheads) correlating to the MRI enhancement and suggesting viable high-grade tumor in these regions. The area of decreased FDG uptake (black arrowheads) corresponds to nonviable tumor.

assessment of tumor and RN.[20,32] Multiple SPECT radiotracers are available for brain tumor imaging in the post-treatment setting. $Thallium^{201}$ concentrates in viable tumor and is highly accurate for post-treatment assessment of tumor burden; however, $Thallium^{201}$ also has nonspecific uptake in non-neoplastic processes such as granulomatous or fungal etiologies.[20,23]

Tc^{99m}MIBI SPECT has improved specificity compared to $Thallium^{201}$, allowing earlier post-treatment tumor assessment and prognostication.[32,33] Unfortunately, MIBI and similar radiotracers (eg, tetrofosmin) demonstrate less uptake and more rapid washout vs $Thallium^{201}$, necessitating higher dosages and shorter imaging intervals for adequate spatial resolution.[32]

As previously discussed, functional/nonfunctional pituitary adenomas,[3] meningiomas, and medulloblastomas express SSRs, thus $Indium^{111}$-pentetreotide may play a role in post-treatment imaging. Medulloblastomas in particular undergo complex treatment regimens often with subtotal resections and combinations of chemotherapy and radiation leading to variable areas of tumor necrosis and gliosis. Due to the high concentrations of SSR-2, $Indium^{111}$-pentetreotide-SPECT can be a useful tool for the evaluation of medulloblastoma recurrence.[3]

PET

In the setting of post-treatment changes, F^{18}-FDG differentiates viable and nonviable tissue, as tumor often shows elevated uptake and RN has no uptake. High-grade tumors typically demonstrate elevated metabolism; however, low-grade entities can also have uptake, including pilocytic astrocytomas and macroadenomas (Fig. 12). Potential pitfalls of FDG-PET include low-grade or mucinous subtype tumors that have low uptake, higher grade tumors with increased anaerobic metabolism as opposed to aerobic metabolism, and false-negative immediate post-treatment scans with FDG uptake on subsequent scans.[4]

Amino acid or nucleoside-based PET radiotracers have high tumor-to-background ratios and are accurate in differentiating tumor recurrence from RN.[6,34] C^{11}-MET PET can identify areas of tumor, although false positives occur as both C^{11}MET and F^{18}-FET can have increased uptake along the periphery of parenchymal hematomas, infarcts, abscesses, and demyelinating lesions.[15]

F^{18}-FLT PET quantitatively measures mitotic activity and identifies recurrent high-grade gliomas with improved prognosis predictions vs F^{18}-FDG PET. F^{18}-FLT uptake is limited by the transportation rate and the BBB.[10] F^{18}-DOPA was initially used for neurodegenerative disorders, but more recently has been found to be accurate in the evaluation of low-grade gliomas, recurrent tumor, and post-treatment changes.[1,10]

Additionally, it is important to keep in mind not only differentiating residual/recurrent tumor from post-treatment changes, but also the importance of assessing for treatment efficacy. There has been specific interest in apoptosis or "programmed cell death." Apoptosis is part of normal homeostasis but also the desired treatment outcome of tumor cells. Many radiotracers have been studied to detect the presence of apoptosis on imaging. 2-(5-Fluoro-pentyl)-2-methyl-

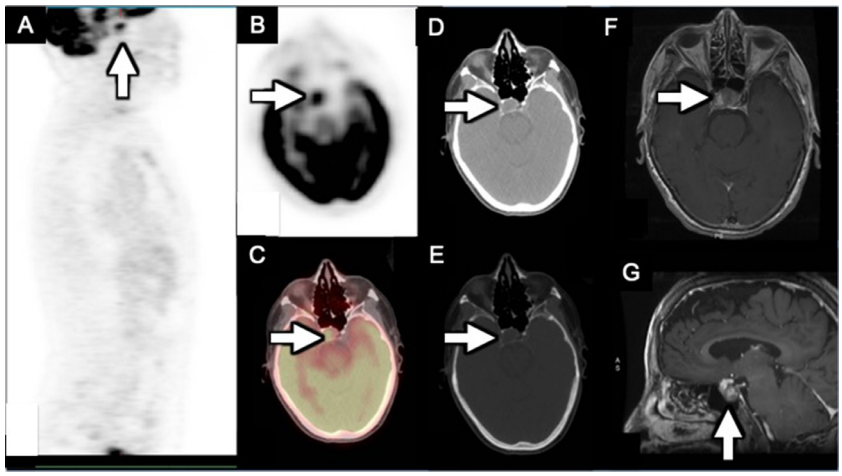

Figure 12 Pituitary macroadenoma on FDG-PET. A 77-year-old woman with right lower lobe lung nodule presents for diagnostic F^{18}-FDG PET-CT. Rotational maximum intensity projection image (A) shows incidental focal increased FDG uptake in the midline skull base (white arrow), which localizes to the sella turcica and pituitary gland on axial PET (B, white arrow) and axial fused PET-CT (C, white arrow) images. Corresponding noncontrast axial CT images in soft tissue (D) and bone algorithm reconstruction (E) show rounded soft tissue and bony expansion/remodeling (white arrows) of the sella turcica. Axial (F) and sagittal (G) postcontrast T1-weighted MR images confirm an enhancing sellar mass (white arrows) consistent with pituitary macroadenoma.

malonic acid (F^{18}-ML-10) targets certain cell membrane processes that occur during apoptosis, resulting in selective transmembrane F^{18}-ML-10 transport into the apoptotic cell. Therefore, F^{18}-ML-10 selectively accumulates within apoptotic cells, and not in viable or necrotic cells. Troubleshooting is required prior to its widespread clinical use, as apoptosis is a transient process requiring particular attention to timing. This timing differs between tumor histologies and treatment methods, with different levels of apoptosis at varying time points[35] (Fig. 13).

SPECT-CT and PET-CT

Studies have shown significant benefits of SPECT and PET radiotracers in the differentiation of residual/recurrent tumor and post-treatment effects.[15] Accuracy is high for differentiating tumor recurrence from RN when recurrence is suspected on anatomic imaging.[32] While PET is the workhorse of oncologic imaging, SPECT is relatively low-cost and widely available with results paralleling PET despite the drawback of poorer spatial resolution.[3] However, hybrid SPECT-CT and PET-CT systems map the morphologic data to the scintigraphic data, thus have the added benefit of better localization of the residual/recurrent tumor and the ability to quantify the amount of viable tumor with prognostication implications.[3] The improved anatomic information is especially crucial where determination of pathologic vs physiologic uptake is challenging (eg, sella turcica).

SPECT-MRI and PET-MRI

MRI is excellent at evaluating neuroanatomy with superior tissue contrast resolution to CT and the added benefit of utilizing multiple imaging sequences to evaluate pathology. Hybrid imaging combines the structural information provided by MRI with the physiologic, biochemical, and molecular information from the NM portion of the exam. Of note, when these studies are completed separately and SPECT/PET is retrospectively fused to MRI sequences, there can be issues from patient re-positioning between imaging acquisitions leading to co-registration problems. These are substantially alleviated with newer hybrid scanners that perform concurrent NM and anatomic imaging.[6] Overall, brain tumor assessment is much improved when the imaging is acquired simultaneously, with a more accurate analysis of tumor location, extent, and grade.[6]

PET-MRI has significantly improved soft-tissue contrast vs PET-CT and is preferred in neuro-oncology.[6] PET-MRI initially focused on PET-CT correlations for primary brain tumor evaluation, but with newer research and development now takes fuller advantage of the complementary MRI and PET data acquired during one imaging session, integrating anatomic, biologic, and metabolic information.[10] Three types of PET-MRI scanner systems are commercially available. First, the tri-modality system is composed of PET-CT and MRI apparatuses, where images are acquired separately and co-registered by software. This system uses the well-established CT-based attenuation correction method; however, there is a large space requirement. Additionally, errors with misregistration can occur due to patient transport between imaging acquisitions. The second category is a sequential system with separate PET and MRI components located in the same room and connected with a single-track table, alleviating misregistration. This system does not utilize CT attenuation correction since there is no CT component. The third category is an integrated system where the PET detector and MRI gantry are combined, and images are acquired simultaneously.[36] Overall, this integrated system minimizes motion

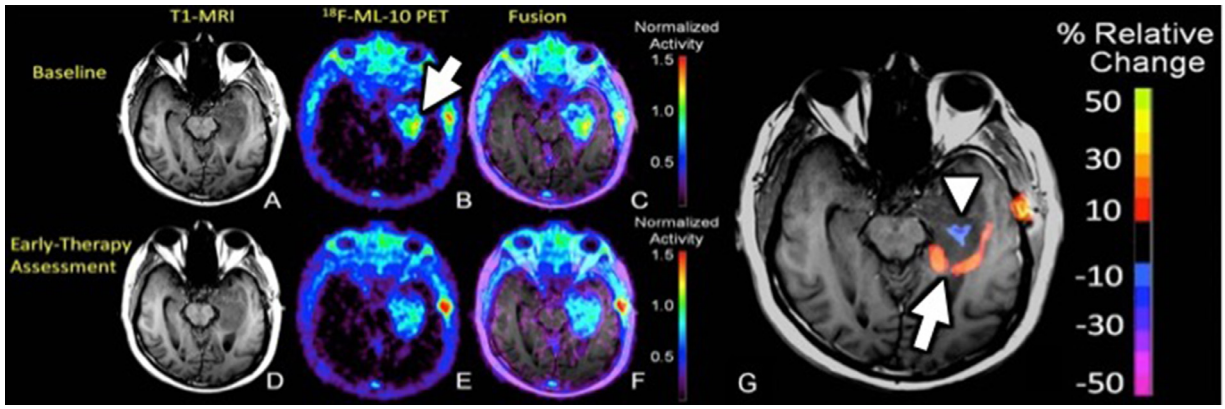

Figure 13 GBM therapy assessment on ML-10 PET. Representative axial T1-weighted MRI and F^{18}-ML-10 PET imaging at baseline (A, B, and C) and early-therapy assessment (ETA; D, E, and F) timepoints in a patient with left temporal lobe GBM. Baseline axial T1-weighted image (A) shows a mass-like region of signal hypointensity in the left mesial temporal lobe. Baseline F^{18}-ML-10 PET (B) shows a corresponding region of high tracer uptake, which localizes to the region of mesial temporal lobe signal abnormality on the PET-MRI fusion image (C). ETA performed following 3 weeks of temozolomide and radiation therapy includes axial T1-weighted MRI (D), axial F^{18}-ML-10 PET (E), and fused PET-MRI (F). Normalized voxel-by-voxel subtraction cluster map of baseline (B) from ETA PET (E) is shown fused to ETA T1-weighted MRI (G), which depicts relative percent changes in F^{18}-ML-10 within the GBM post-treatment. Note that some regions of the GBM exhibiting high baseline F^{18}-ML-10 uptake now show reduced uptake at ETA (white arrowhead), but there are new regions (compared to baseline) of F^{18}-ML-10 uptake present at the tumor periphery (white arrow), which indicate a mixed response to therapy.[39] Adapted with permission from "First use of (18)F-labeled ML-10 PET to assess apoptosis change in a newly diagnosed glioblastoma multiforme patient before and early after therapy" by Oborski MJ et al, 2014, *Brain Behav,* 4(2):312-315.

correction and has better anatomic correlation, improved co-registration, and more accurate detection of recurrent tumor vs RN.[6,10,36] Improvement in anatomic localization aids in biopsy planning, estimates of gross-tumor volume, and assessments of tumor margins for radiation planning.[36]

Conclusion

Brain tumors are a heterogeneous group of entities, for which neuroimaging plays a pivotal role regarding diagnosis, grading, treatment response, and evaluation of complications. Continued advancements in treatment result in challenging interpretations of post-treatment neuroimaging. CT and MRI provide anatomic data, while SPECT and PET provide physiologic/molecular data beyond what is possible through anatomic imaging alone. The integrated information acquired from these studies individually or via hybrid systems contributes to more accurate tumor grading, analysis of tumor location/extent, delineation of tumor margins, treatment planning, post-treatment assessment, and prognosis.

References

1. Mabray MC, Barajas RF, Cha S: Modern brain tumor imaging. Brain Tumor Res Treat 3:8-23, 2015. https://doi.org/10.14791/btrt.2015.3.1.8. [published Online First: Epub Date]
2. Filippi L, Santoni R, Manni C, et al: Imaging primary brain tumors by SPECT with Technetium-99m Sestamibi (MIBI) and Tetrofosmin. Curr Med Imaging 1:61-66, 2005
3. Schillaci O, Filippi L, Manni C, et al: Single-photon emission computed tomography/computed tomography in brain tumors. Semin Nucl Med 37:34-47, 2007. https://doi.org/10.1053/j.semnuclmed.2006.08.003. [published Online First: Epub Date]
4. Langleben DD, Segall GM: PET in differentiation of recurrent brain tumor from radiation injury. J Nucl Med 41:1861-1867, 2000
5. Essig M, Anzalone N, Combs SE, et al: MR imaging of neoplastic central nervous system lesions: Review and recommendations for current practice. AJNR Am J Neuroradiol 33:803-817, 2012. https://doi.org/10.3174/ajnr.A2640. [published Online First: Epub Date]
6. Heiss WD, Raab P, Lanfermann H: Multimodality assessment of brain tumors and tumor recurrence. J Nucl Med 52:1585-1600, 2011. https://doi.org/10.2967/jnumed.110.084210. [published Online First: Epub Date]
7. Wang LL, Leach JL, Breneman JC, et al: Critical role of imaging in the neurosurgical and radiotherapeutic management of brain tumors. Radiographics 34:702-721, 2014. https://doi.org/10.1148/rg.343130156. [published Online First: Epub Date]
8. Ullrich RT, Kracht LW, Jacobs AH: Neuroimaging in patients with gliomas. Semin Neurol 28:484-494, 2008. https://doi.org/10.1055/s-0028-1083696. [published Online First: Epub Date]
9. Drevelegas A, Papanikolaou N: Imaging modalities in brain tumors. In: Drevelegas A (ed): Imaging of Brain Tumors With Histological Correlations, Springer, 13-24, 2011
10. Fink JR, Muzi M, Peck M, et al: Multimodality brain tumor imaging: MR imaging, PET, and PET/MR imaging. J Nucl Med 56:1554-1561, 2015. https://doi.org/10.2967/jnumed.113.131516. [published Online First: Epub Date]
11. Nuclear Medicine. National Institute of Biomedical Imaging and Bioengineering. Retrieved May 10, 2020, from https://www.nibib.nih.gov/science-education/science-topics/nuclear-medicine#:~:text=
12. Brandon D, Alazraki A, Halkar RK, et al: The role of single-photon emission computed tomography and SPECT/computed tomography in oncologic imaging. Semin Oncol 38:87-108, 2011. https://doi.org/10.1053/j.seminoncol.2010.11.003. [published Online First: Epub Date]
13. Histed SN, Lindenberg ML, Mena E, et al: Review of functional/anatomical imaging in oncology. Nucl Med Commun 33:349-361, 2012. https://doi.org/10.1097/MNM.0b013e32834ec8a5. [published Online First: Epub Date]

14. Townsend DW: Combined positron emission tomography-computed tomography: The historical perspective. Semin Ultrasound CT MR 29 (4):232-235, 2008. https://doi.org/10.1053/j.sult.2008.05.006. [published Online First: Epub Date]
15. Herholz K, Langen KJ, Schiepers C, et al: Brain tumors. Semin Nucl Med 42:356-370, 2012. https://doi.org/10.1053/j.semnuclmed.2012.06.001. [published Online First: Epub Date]
16. Johnson DR, Guerin JB, Giannini C, et al: 2016 updates to the WHO brain tumor classification system: What the radiologist needs to know. Radiographics 37:2164-2180, 2017. https://doi.org/10.1148/rg.2017170037. [published Online First: Epub Date]
17. Hutton BF: The origins of SPECT and SPECT/CT. Eur J Nucl Med Mol Imaging 41(suppl 1):S3-16, 2014. https://doi.org/10.1007/s00259-013-2606-5. [published Online First: Epub Date]
18. Dierckx RA, Martin JJ, Dobbeleir A, et al: Sensitivity and specificity of thallium-201 single-photon emission tomography in the functional detection and differential diagnosis of brain tumours. Eur J Nucl Med 21:621-633, 1994. https://doi.org/10.1007/bf00285584. [published Online First: Epub Date]
19. Biersack HJ, Grünwald F, Kropp J: Single photon emission computed tomography imaging of brain tumors. Semin Nucl Med 21:2-10, 1991. https://doi.org/10.1016/s0001-2998(05)80075-3. [published Online First: Epub Date]
20. Lorberboym M, Baram J, Feibel M, et al: A prospective evaluation of thallium-201 single photon emission computerized tomography for brain tumor burden. Int J Radiat Oncol Biol Phys 32:249-254, 1995. https://doi.org/10.1016/0360-3016(95)00580-R. [published Online First: Epub Date]
21. Kuwert T, Woesler B, Morgenroth C, et al: Diagnosis of recurrent glioma with SPECT and iodine-123-alpha-methyl tyrosine. J Nucl Med 39:23-27, 1998
22. Galldiks N, Lohmann P, Albert NL, et al: Current status of PET imaging in neuro-oncology. Neurooncol Adv 1:1-11, 2019.
23. Lee JD, Kim DI, Lee JT, et al: Indium-111-pentetreotide imaging in intra-axial brain tumors: Comparison with thallium-201 SPECT and MRI. J Nucl Med 36:537-541, 1995
24. Herholz K: Brain tumors: An update on clinical PET research in gliomas. Semin Nucl Med 47:5-17, 2017. https://doi.org/10.1053/j.semnuclmed.2016.09.004. [published Online First: Epub Date]
25. Yordanova A, Eppard E, Kürpig S, et al: Theranostics in nuclear medicine practice. Oncol Targets Ther 10:4821-4828, 2017. https://doi.org/10.2147/OTT.S140671. [published Online First: Epub Date]
26. Villanueva-Meyer JE, Mabray MC, Cha S: Current clinical brain tumor imaging. Neurosurgery 81:397-415, 2017. https://doi.org/10.1093/neuros/nyx103. [published Online First: Epub Date]
27. Kessler AT, Bhatt AA: Brain tumour post-treatment imaging and treatment-related complications. Insights Imaging 9:1057-1075, 2018. https://doi.org/10.1007/s13244-018-0661-y. [published Online First: Epub Date]
28. Cha S: Update on brain tumor imaging: From anatomy to physiology. AJNR Am J Neuroradiol 27:475-487, 2006
29. Shah R, Vattoth S, Jacob R, et al: Radiation necrosis in the brain: Imaging features and differentiation from tumor recurrence. Radiographics 32:1343-1359, 2012. https://doi.org/10.1148/rg.325125002. [published Online First: Epub Date]
30. Hygino da Cruz LC, Rodriguez I, Domingues RC, et al: Pseudoprogression and pseudoresponse: Imaging challenges in the assessment of posttreatment glioma. AJNR Am J Neuroradiol 32:1978-1985, 2011. https://doi.org/10.3174/ajnr.A2397. [published Online First: Epub Date]
31. Wen PY, Chang SM, Van den Bent MJ, et al: Response assessment in neuro-oncology clinical trials. J Clin Oncol 35:2439-2449, 2017. https://doi.org/10.1200/JCO.2017.72.7511. [published Online First: Epub Date]
32. Zhang H, Ma L, Wu C, et al: Performance of SPECT in the differential diagnosis of glioma recurrence from radiation necrosis. J Clin Neurosci 22:229-237, 2015. https://doi.org/10.1016/j.jocn.2014.06.102. [published Online First: Epub Date]
33. Beauchesne P, Pedeux R, Boniol M, et al: 99mTc-sestamibi brain SPECT after chemoradiotherapy is prognostic of survival in patients with high-grade glioma. J Nucl Med 45:409-413, 2004
34. Giovacchini G, Riondato M, Giovannini E, et al: Diagnostic applications of nuclear medicine: Brain tumors. Nucl Oncol 2017. Springer, Cham
35. Demirci E, Ahmed R, Ocak M, et al: Preclinical Evaluation of. Mol Imaging 16 https://doi.org/10.1177/1536012116685941, 2017. [published Online First: Epub Date]
36. Rosenkrantz AB, Friedman K, Chandarana H, et al: Current status of hybrid PET/MRI in oncologic imaging. AJR Am J Roentgenol 206:162-172, 2016. https://doi.org/10.2214/AJR.15.14968. [published Online First: Epub Date]
37. Oborski MJ, Demirci E, Laymon CM, et al: Assessment of early therapy response with 18F-FLT PET in glioblastoma multiforme. Clin Nucl Med 39:e431-e432, 2014. https://doi.org/10.1097/RLU.0000000000000321. [published Online First: Epub Date]
38. Oborski MJ, Laymon CM, Lieberman FS, et al: Distinguishing pseudoprogression from progression in high-grade gliomas: A brief review of current clinical practice and demonstration of the potential value of 18F-FDG PET. Clin Nucl Med 38:381-384, 2013. https://doi.org/10.1097/RLU.0b013e318286c148. [published Online First: Epub Date]
39. Oborski MJ, Laymon CM, Lieberman FS, et al: First use of (18)F-labeled ML-10 PET to assess apoptosis change in a newly diagnosed glioblastoma multiforme patient before and early after therapy. Brain Behav 4:312-315, 2014. https://doi.org/10.1002/brb3.217. [published Online First: Epub Date]